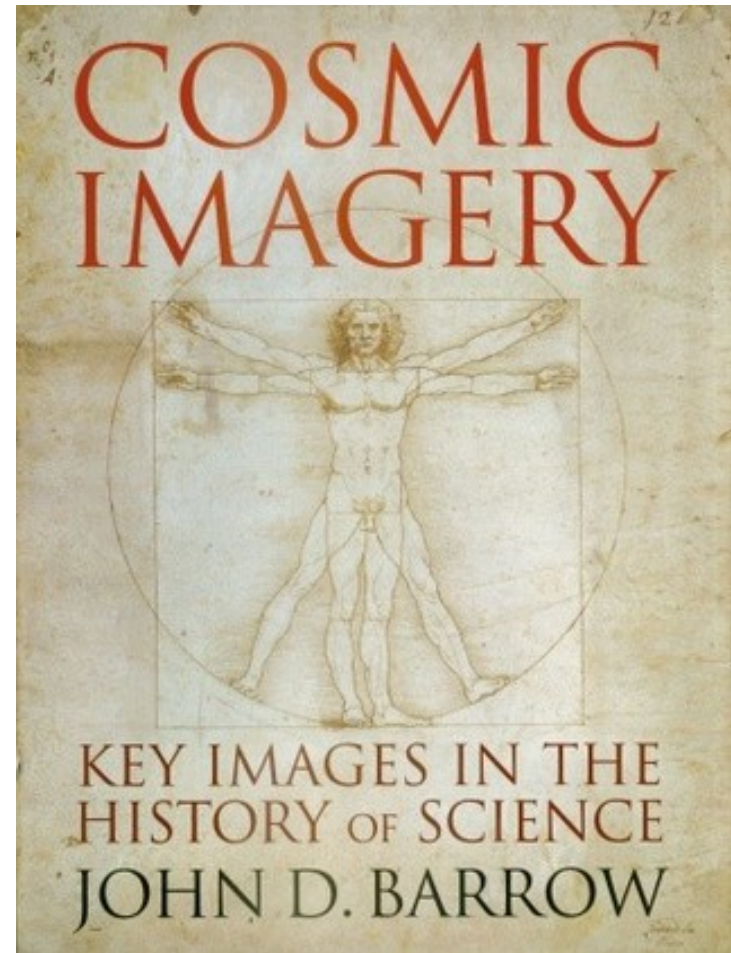
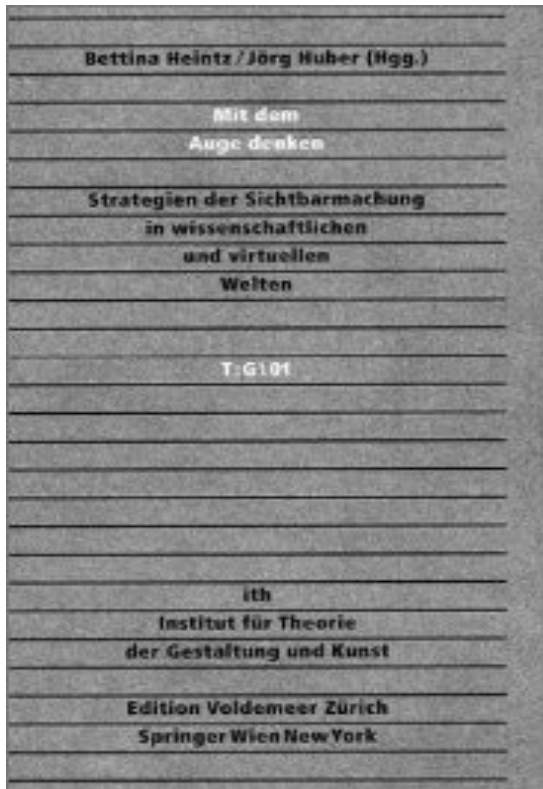


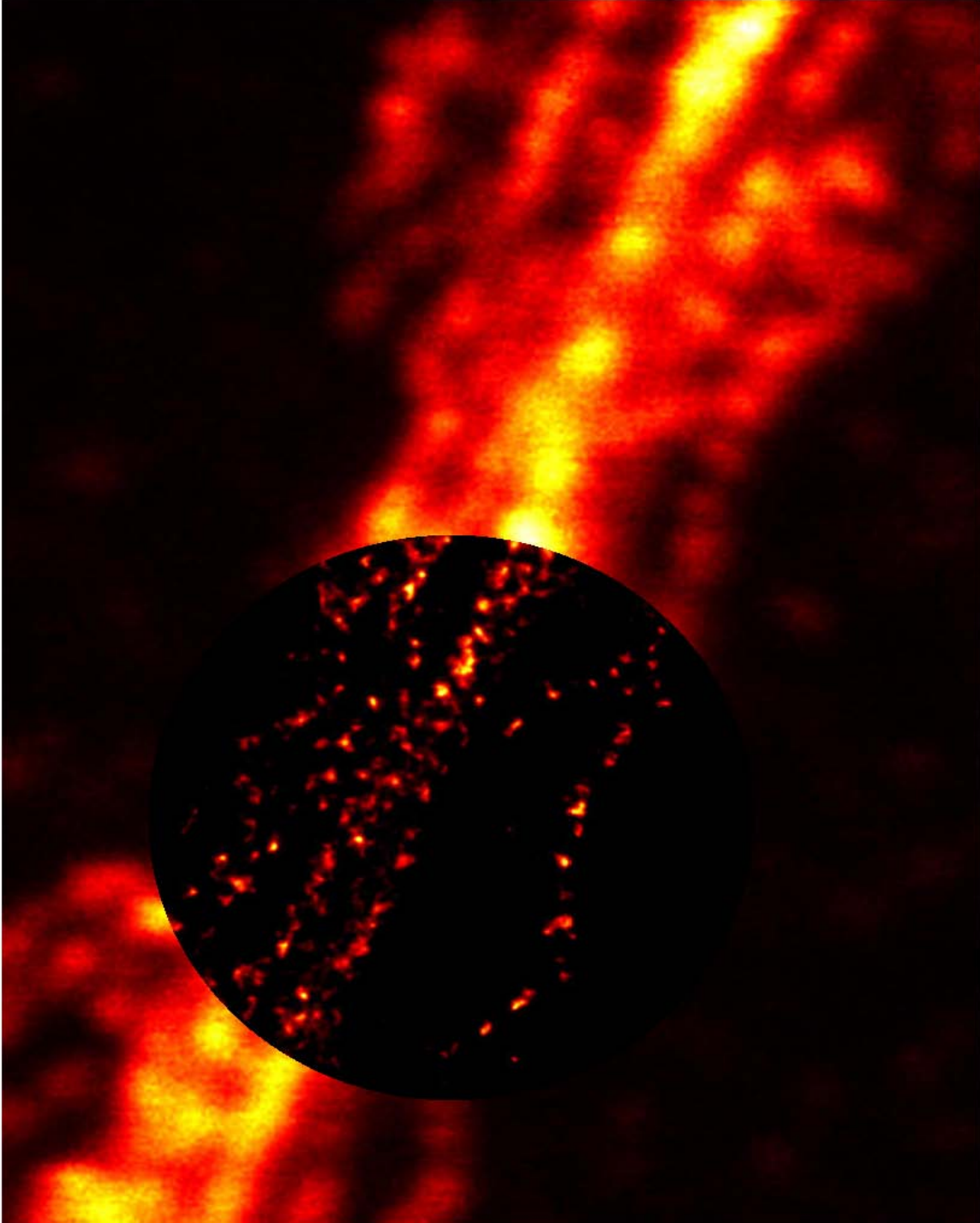
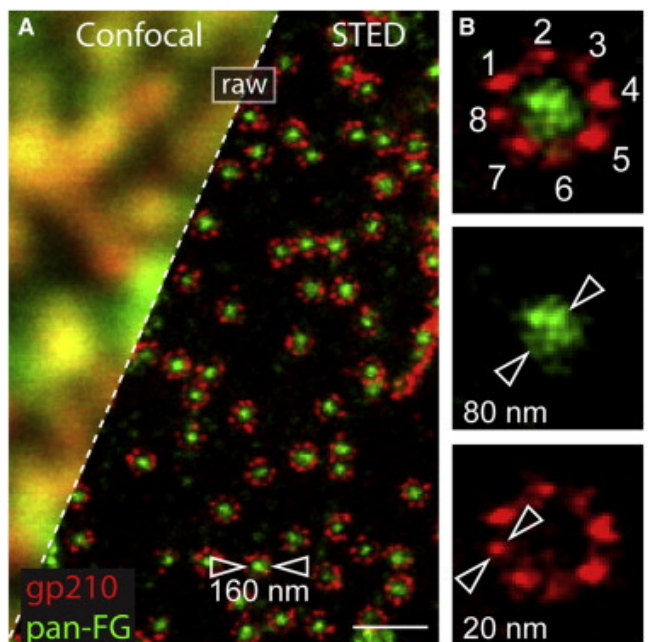
Ernst Peter Fischer
Konstanz, November 2014

Mit dem Auge denken

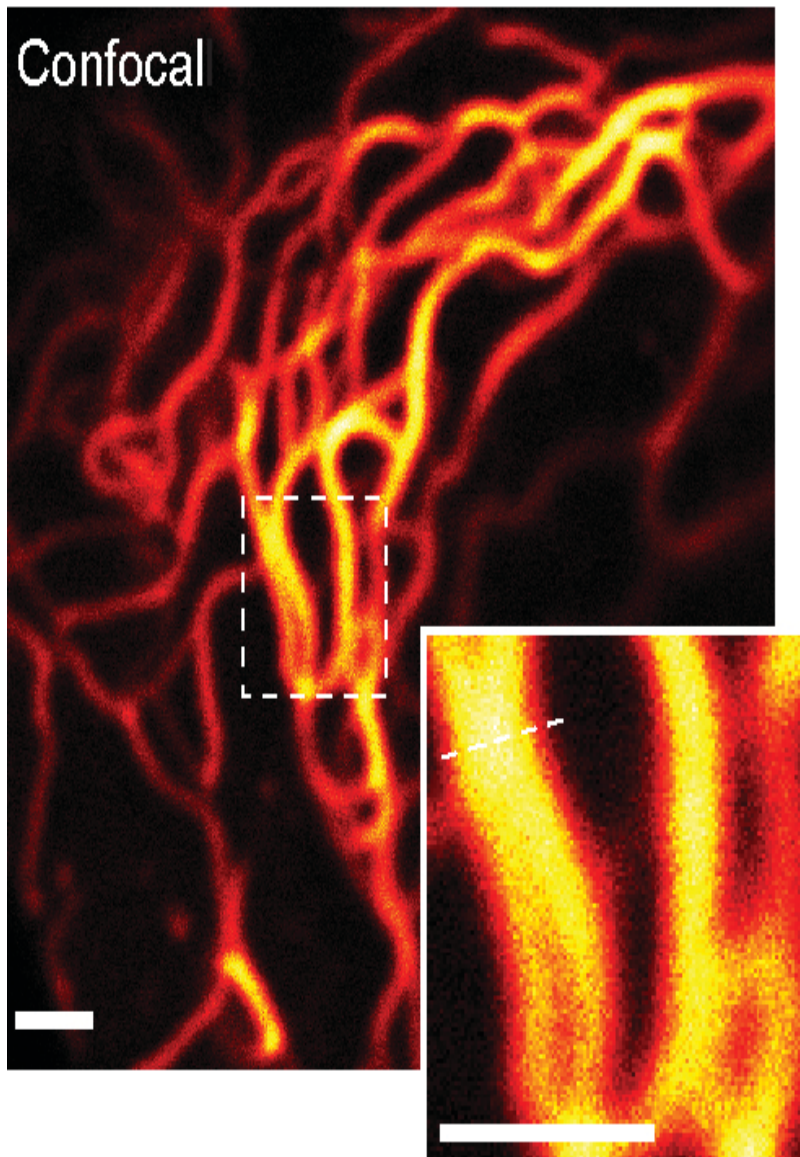
Die Rolle von Bildern in den
Naturwissenschaften

Bücher zu den Bildern

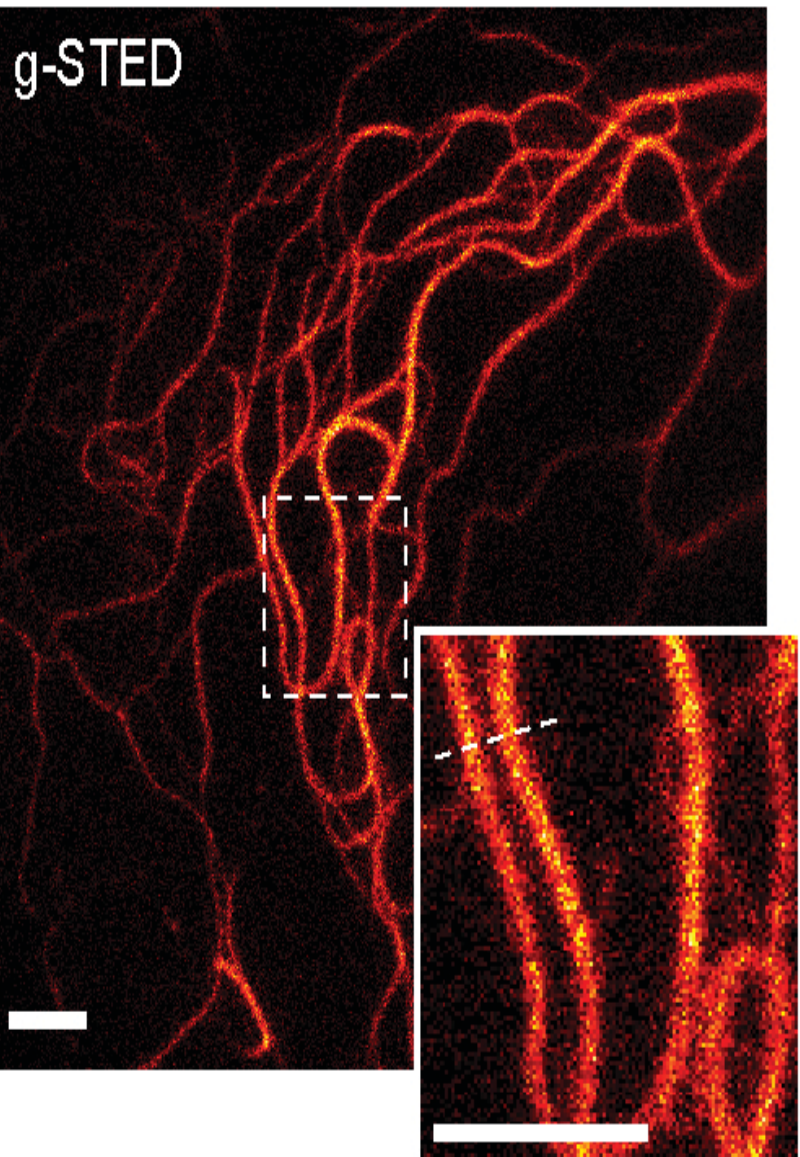




Confocal



g-STED





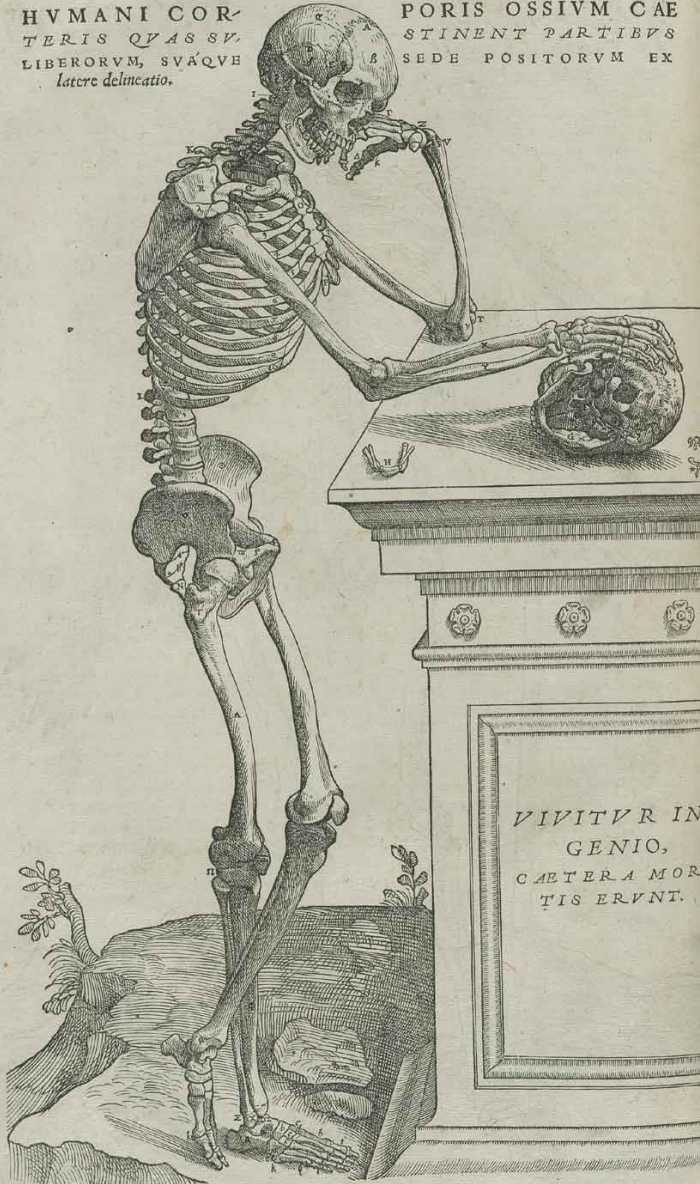
NICOLAI COPERNICCI

net, in quo terram cum orbe lunari tanquam epicyclo contineri diximus. Quinto loco Venus nono mense reducitur. Sextum deniq; locum Mercurius tenet, octuaginta dierum spacio circu currens, In medio uero omnium residet Sol. Quis enim in hoc



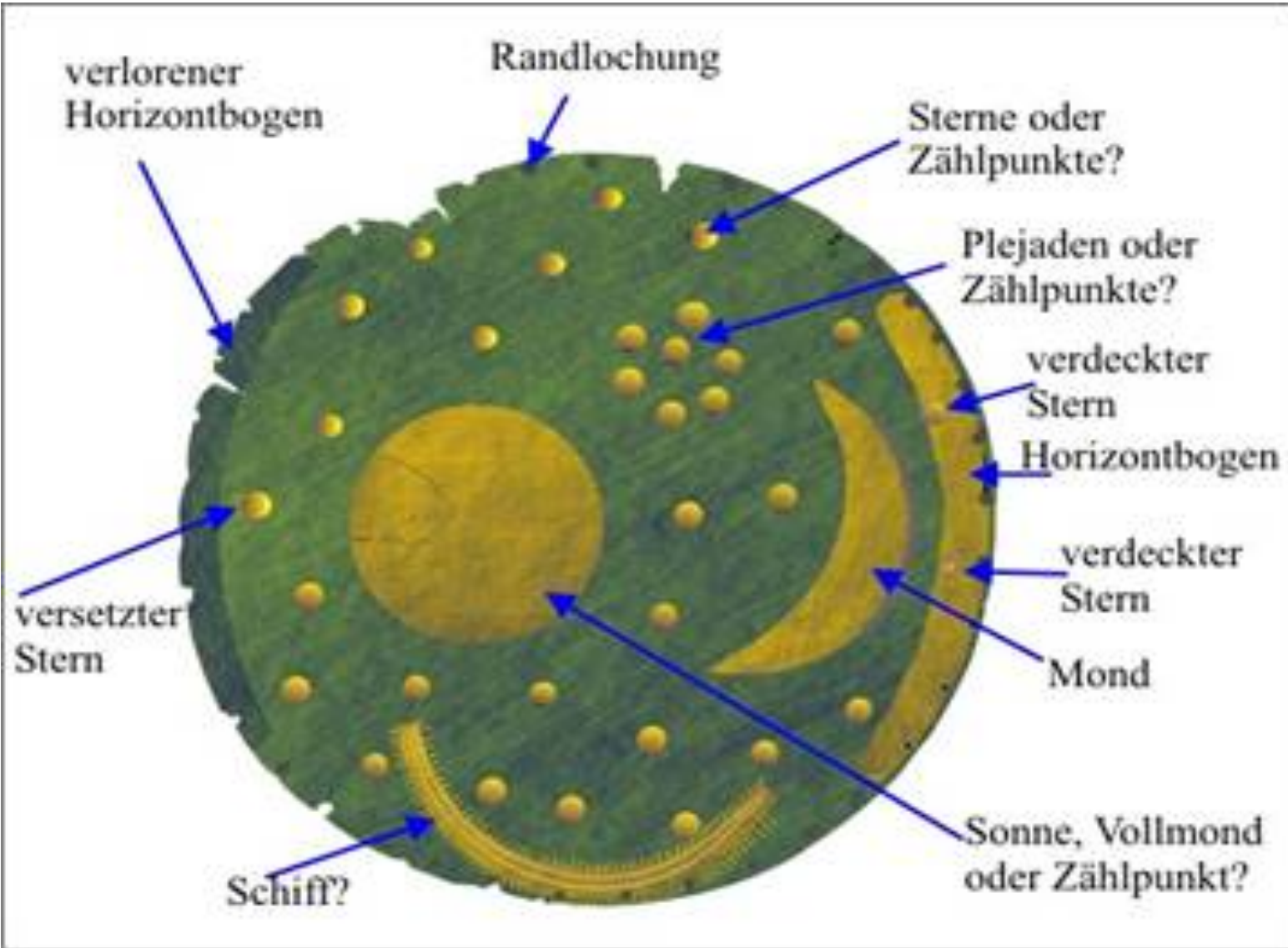
pulcherimo templo lampadem hanc in alio uel meliori loco poseret, quam unde totum simus possit illuminare? Siquidem non incepit quidam lucernam mundi, alijs mentem, alijs rectorem uocant. Trimegistus uisibilem Deum, Sophodis Electra intuentem omnia. Ita profecto tanquam in folio regali Sol residens circum agentem gubernat Astrorum familiam. Tellus quoq; minime fraudatur lunari ministerio, sed ut Aristoteles de animalibus ait, maximā Luna cū terra cognitionē habet. Concipit interea à Sole terra, & impregnatur annuo partu. Inuenimus igitur sub hac

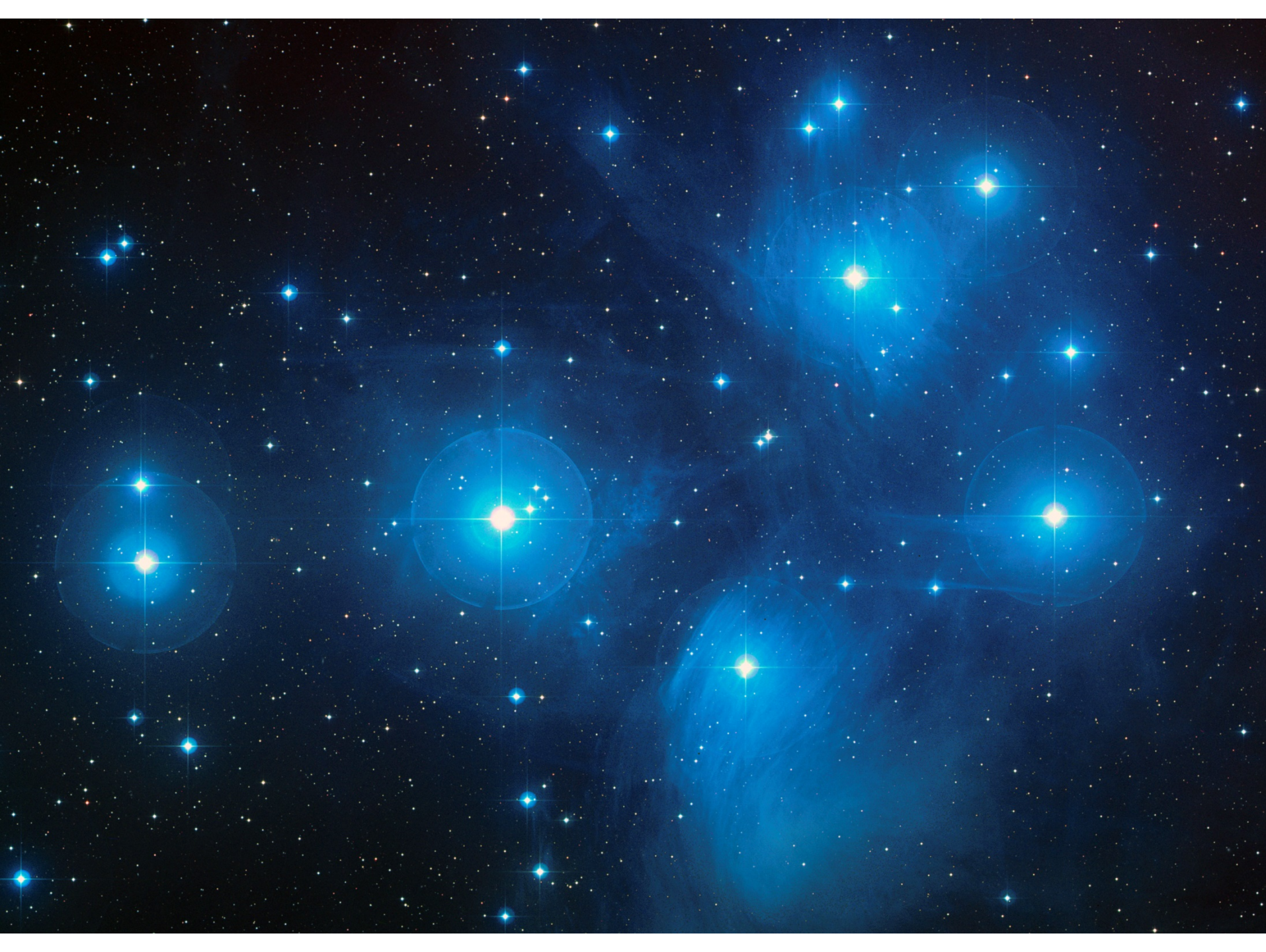
ANDRÉAE VESALII BRUXELLENsis
HUMANI COR-
TERIS QVAS SV-
LIBERORVM, SVĀQVE
latere delineatio.







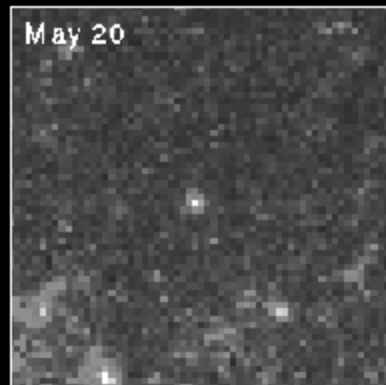
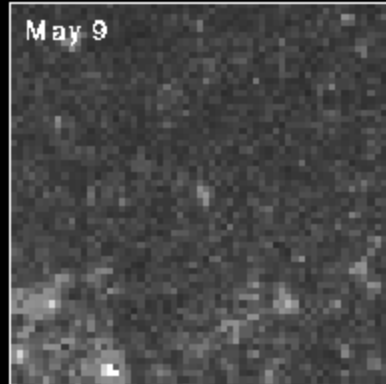
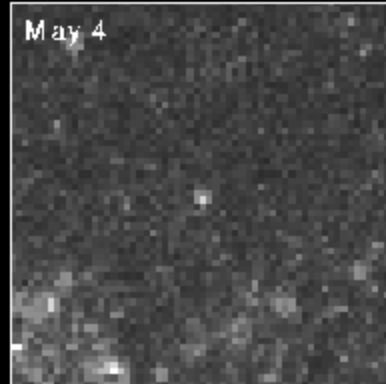
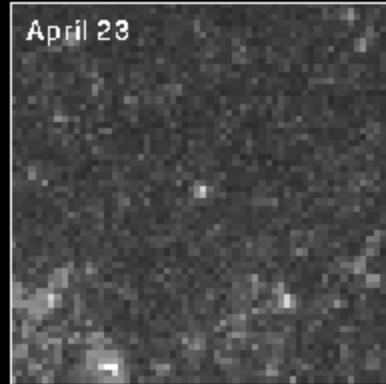






Cepheid Variable Star in Galaxy M100

HST-WFPC2



332H ICM 2-3-2-0 + 2 pioneer 08-2-2-4
380:3 photos AH

~~N~~
YAR!

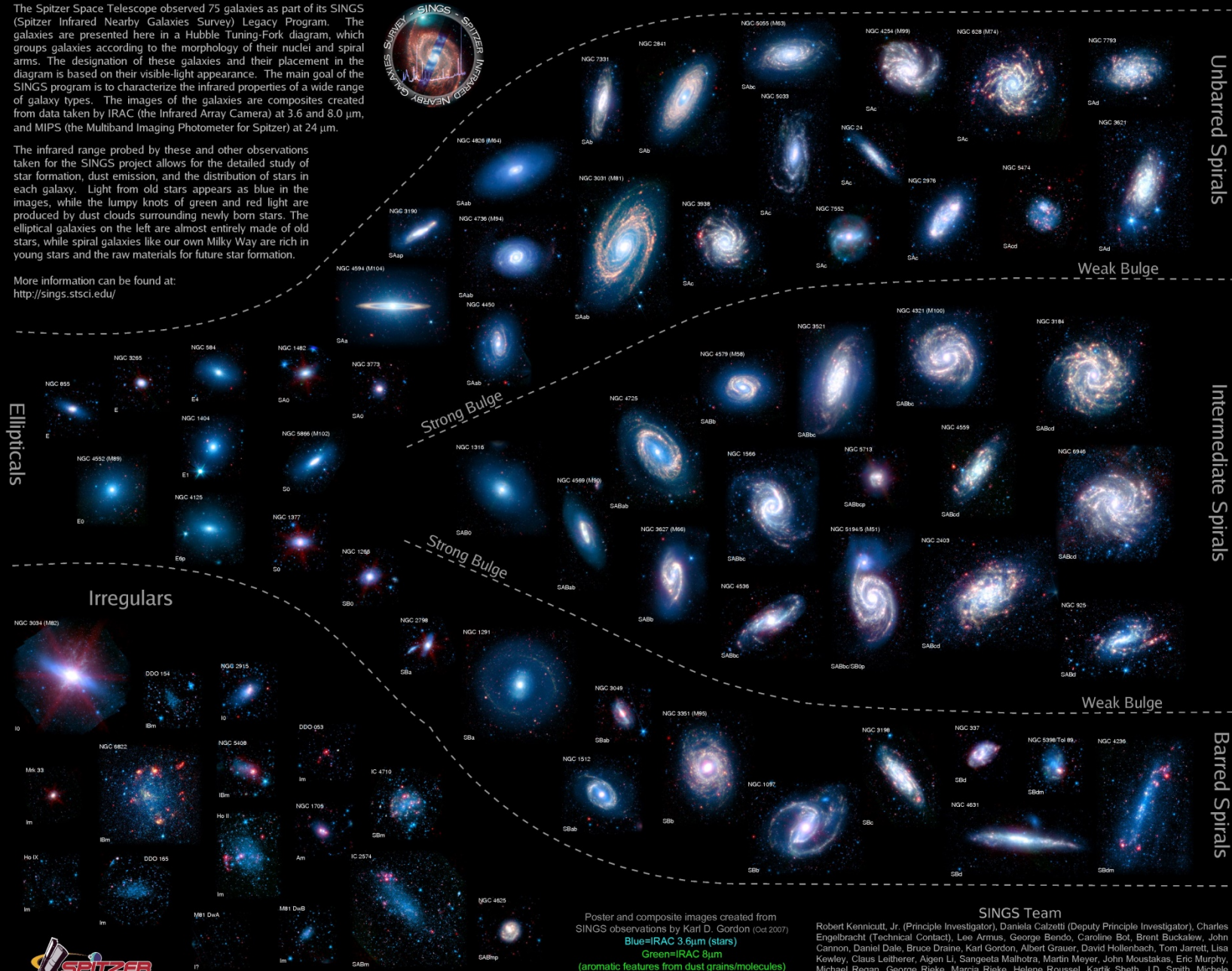
6-Oct
1923

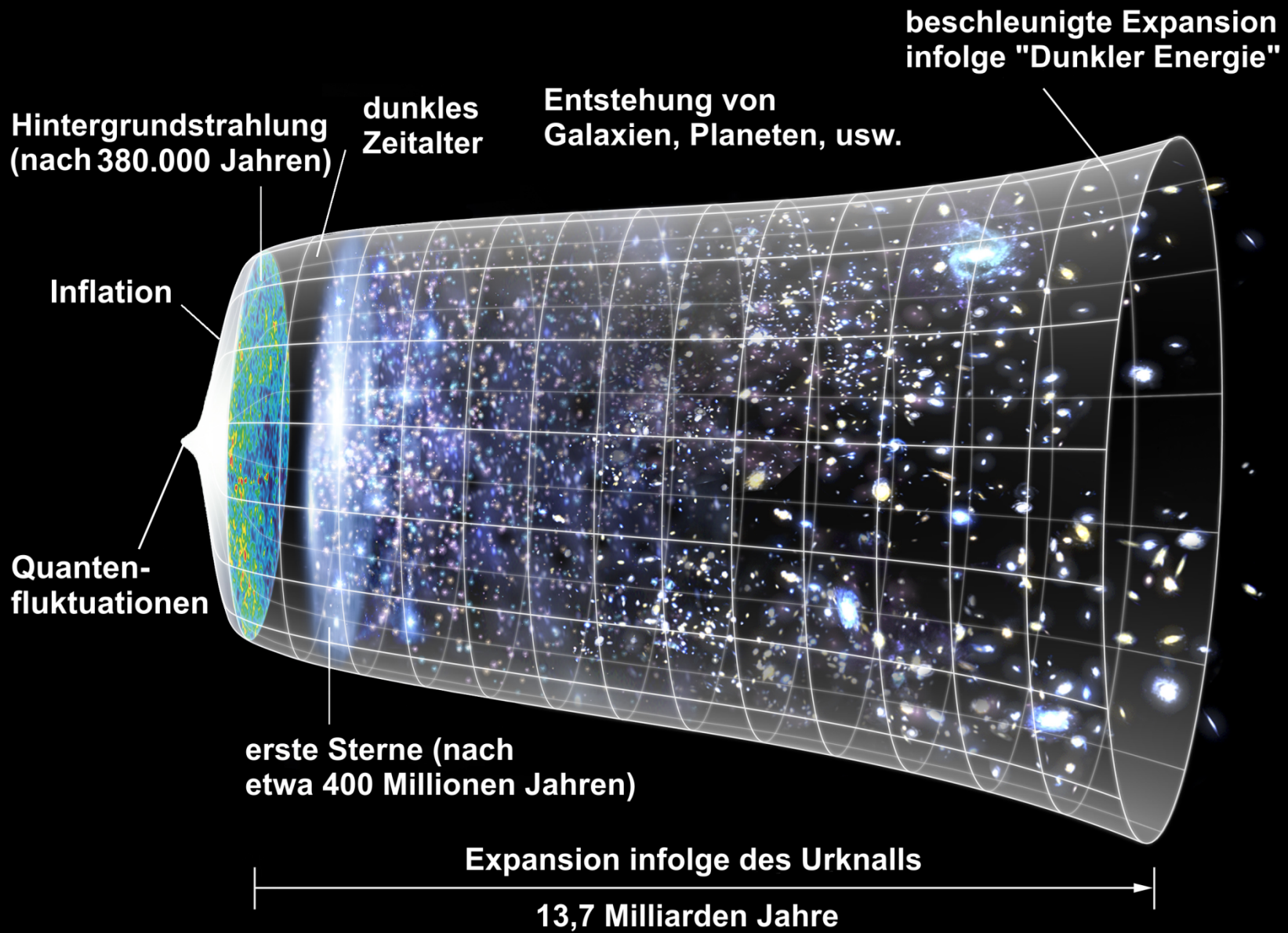
The Spitzer Infrared Nearby Galaxies Survey (SINGS) Hubble Tuning-Fork

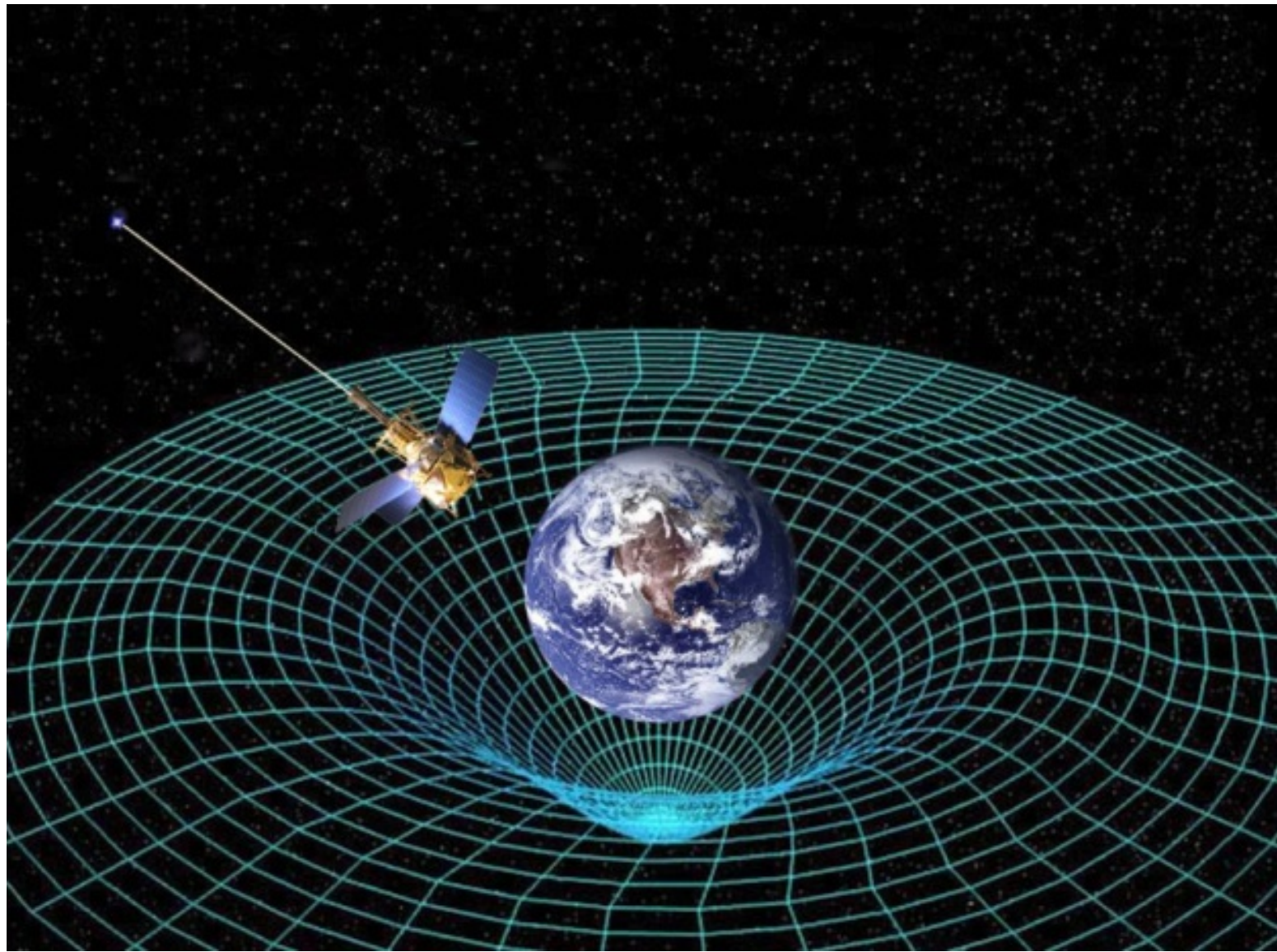
The Spitzer Space Telescope observed 75 galaxies as part of its SINGS (Spitzer Infrared Nearby Galaxies Survey) Legacy Program. The galaxies are presented here in a Hubble Tuning-Fork diagram, which groups galaxies according to the morphology of their nuclei and spiral arms. The designation of these galaxies and their placement in the diagram is based on their visible-light appearance. The main goal of the SINGS program is to characterize the infrared properties of a wide range of galaxy types. The images of the galaxies are composites created from data taken by IRAC (the Infrared Array Camera) at 3.6 and 8.0 μm , and MIPS (the Multiband Imaging Photometer for Spitzer) at 24 μm .

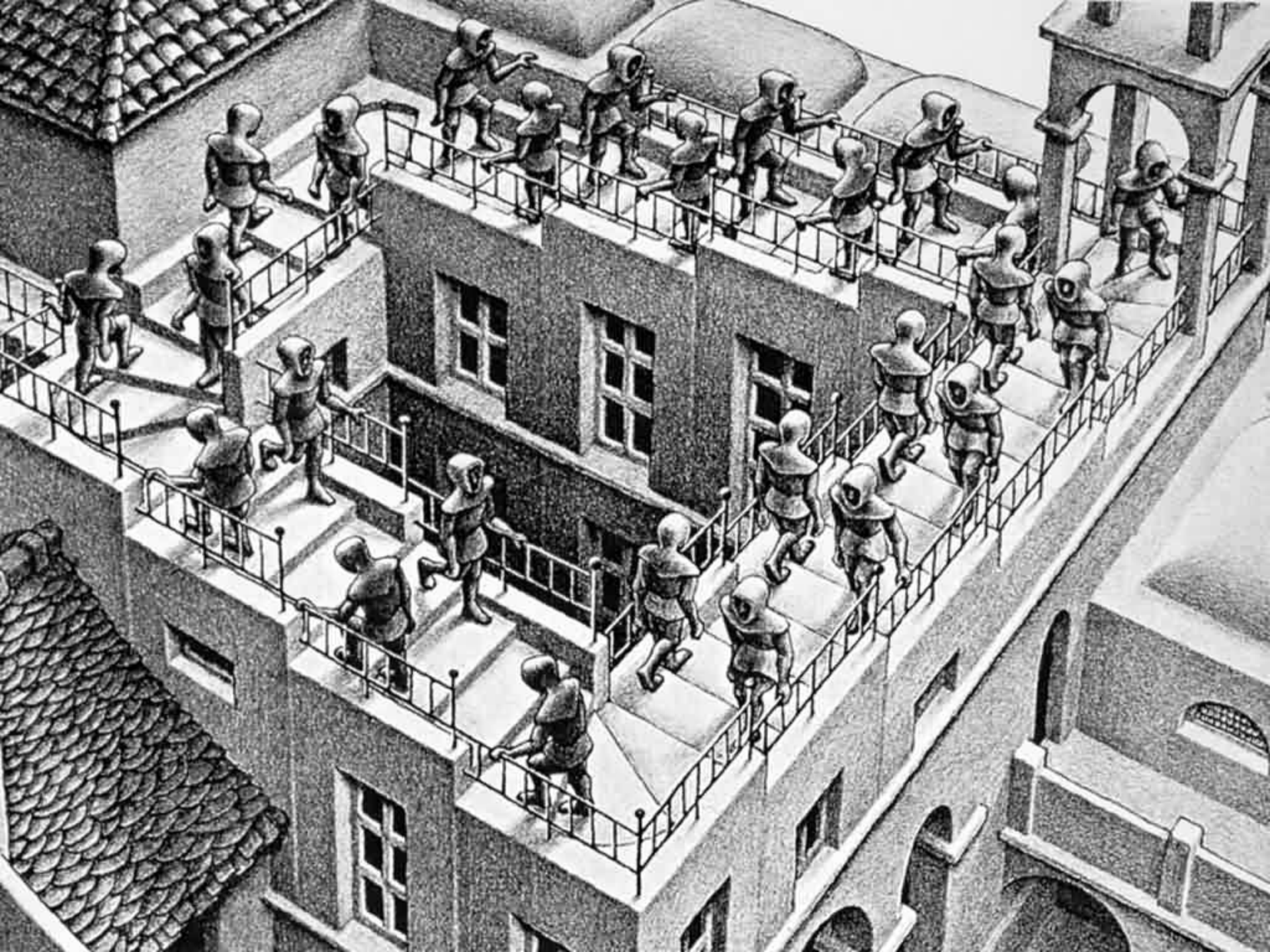
The infrared range probed by these and other observations taken for the SINGS project allows for the detailed study of star formation, dust emission, and the distribution of stars in each galaxy. Light from old stars appears as blue in the images, while the lumpy knots of green and red light are produced by dust clouds surrounding newly born stars. The elliptical galaxies on the left are almost entirely made of old stars, while spiral galaxies like our own Milky Way are rich in young stars and the raw materials for future star formation.

More information can be found at:
<http://sings.stsci.edu/>







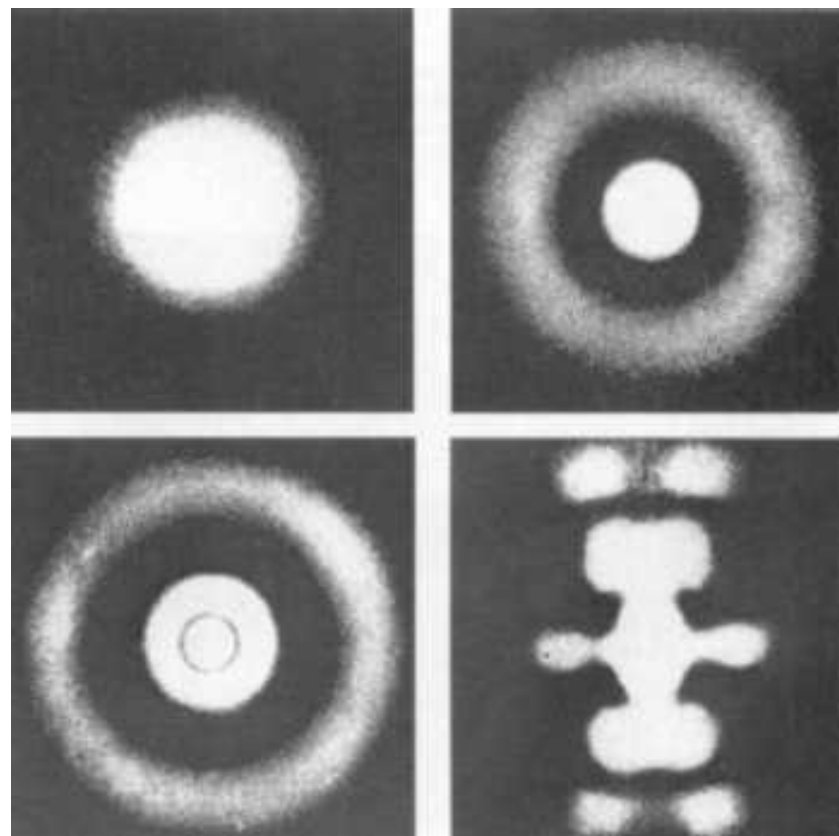
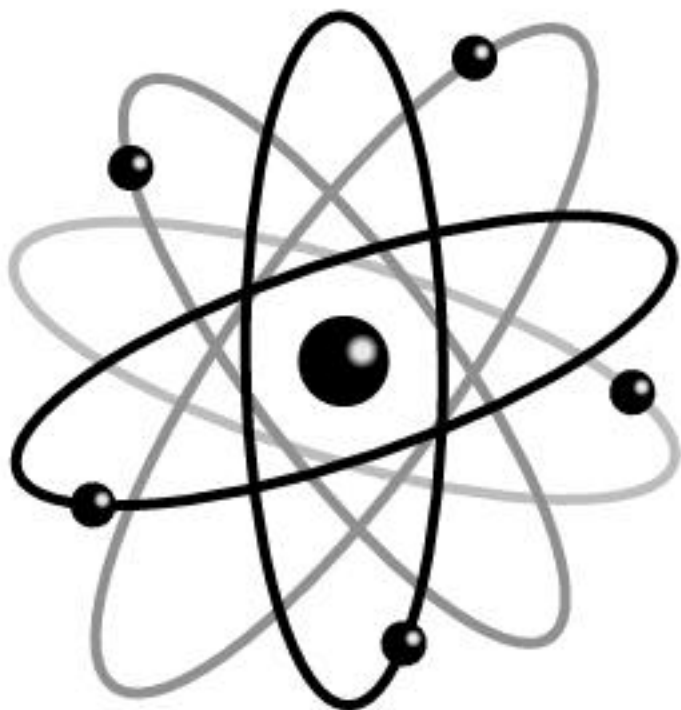


Les Demoiselles d'Avignon (1907)

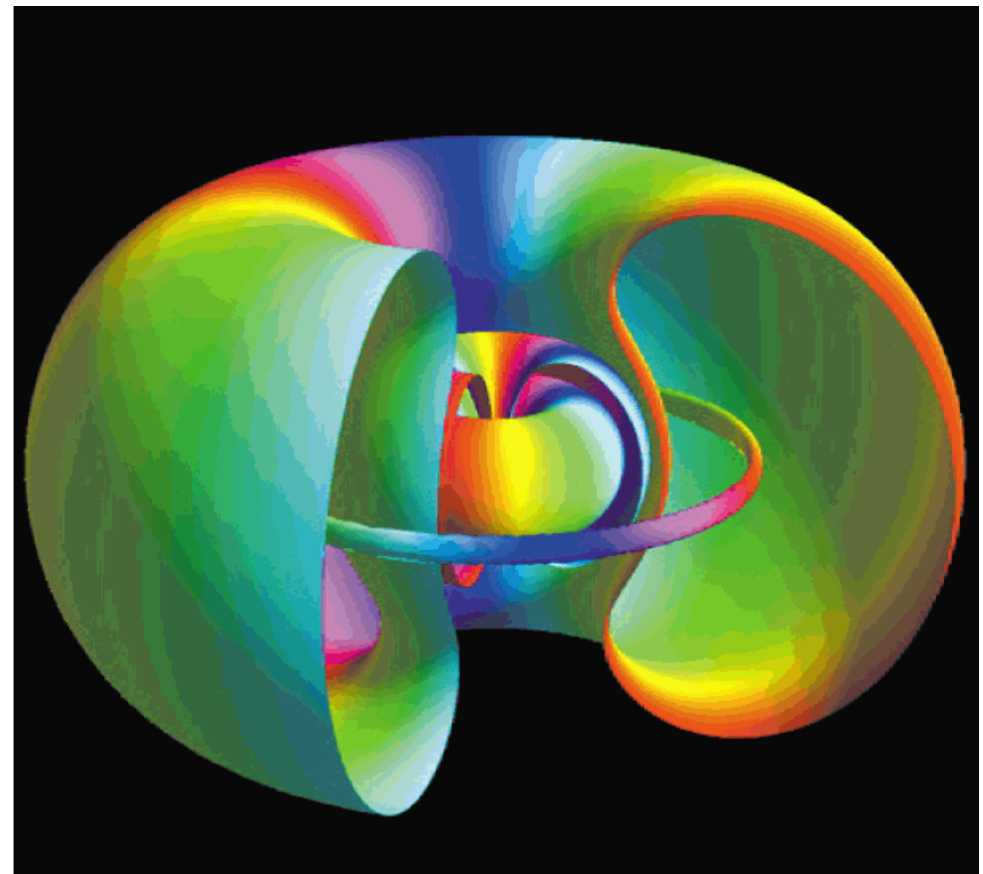
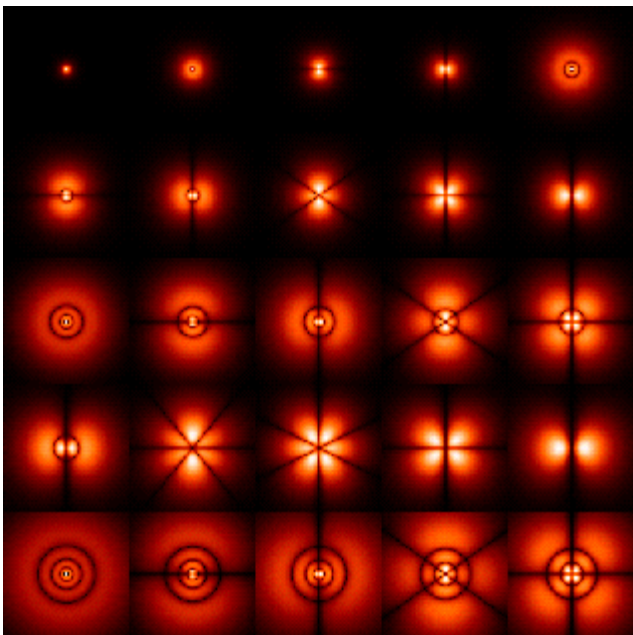


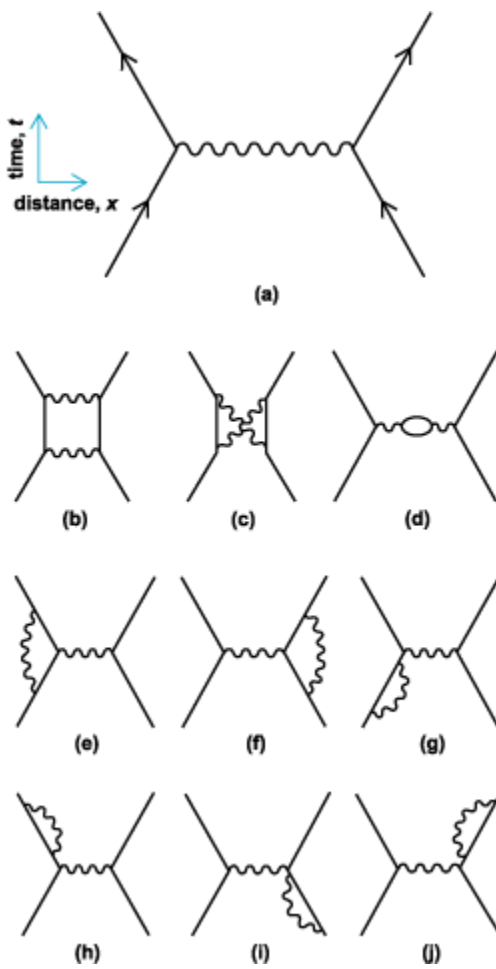
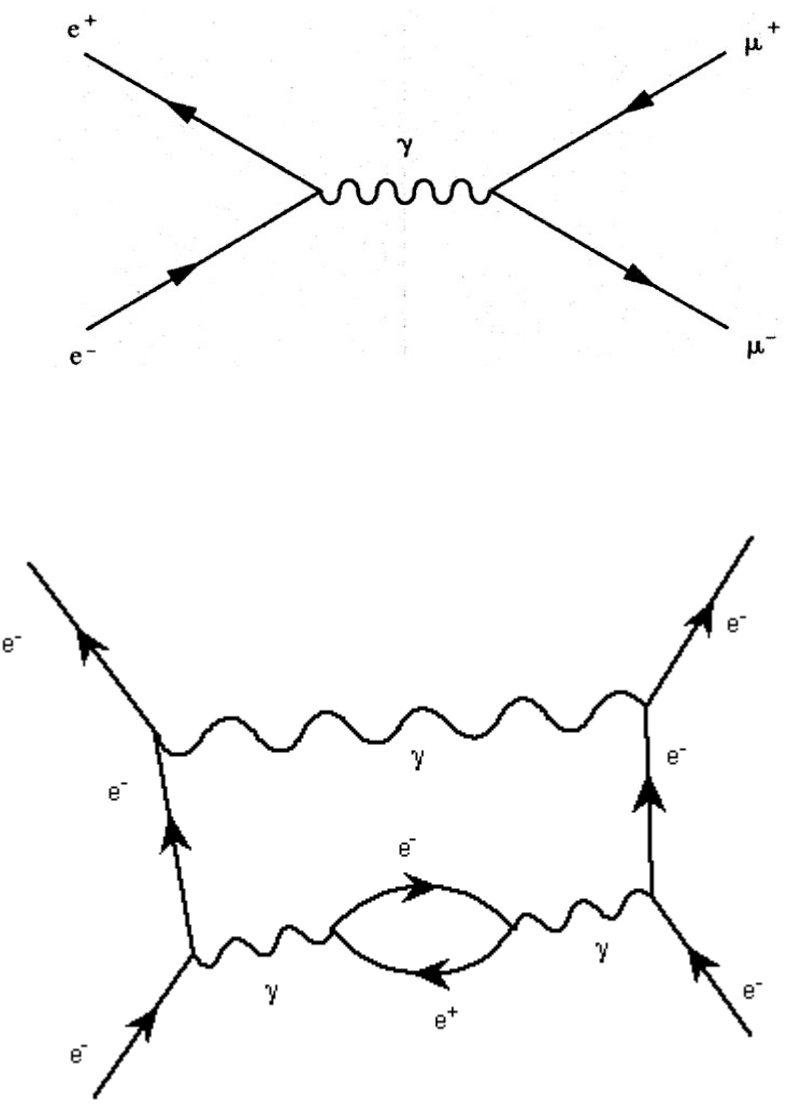


Das Bild der Atome

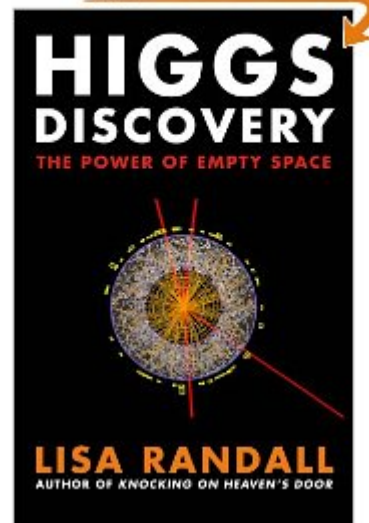
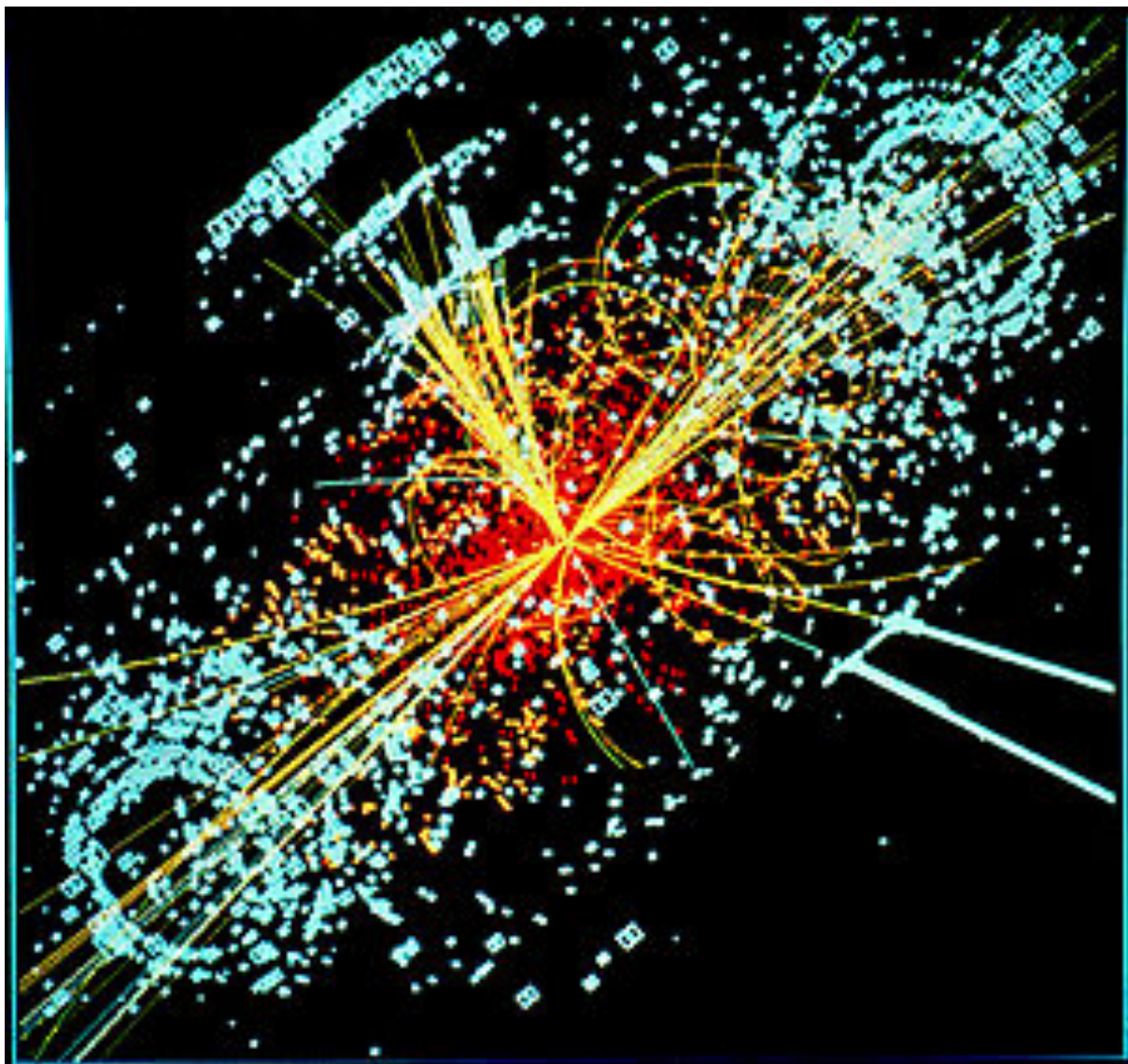


Atomphysik (20. Jahrhundert) – Mathematik als Kunst

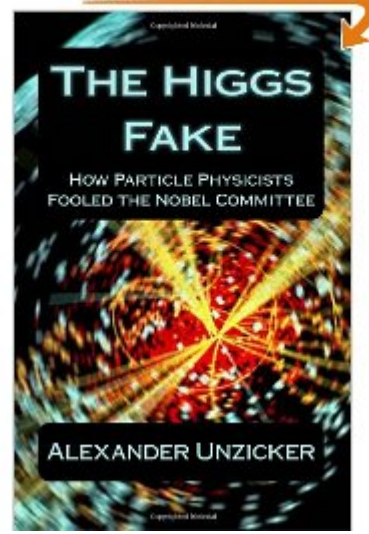


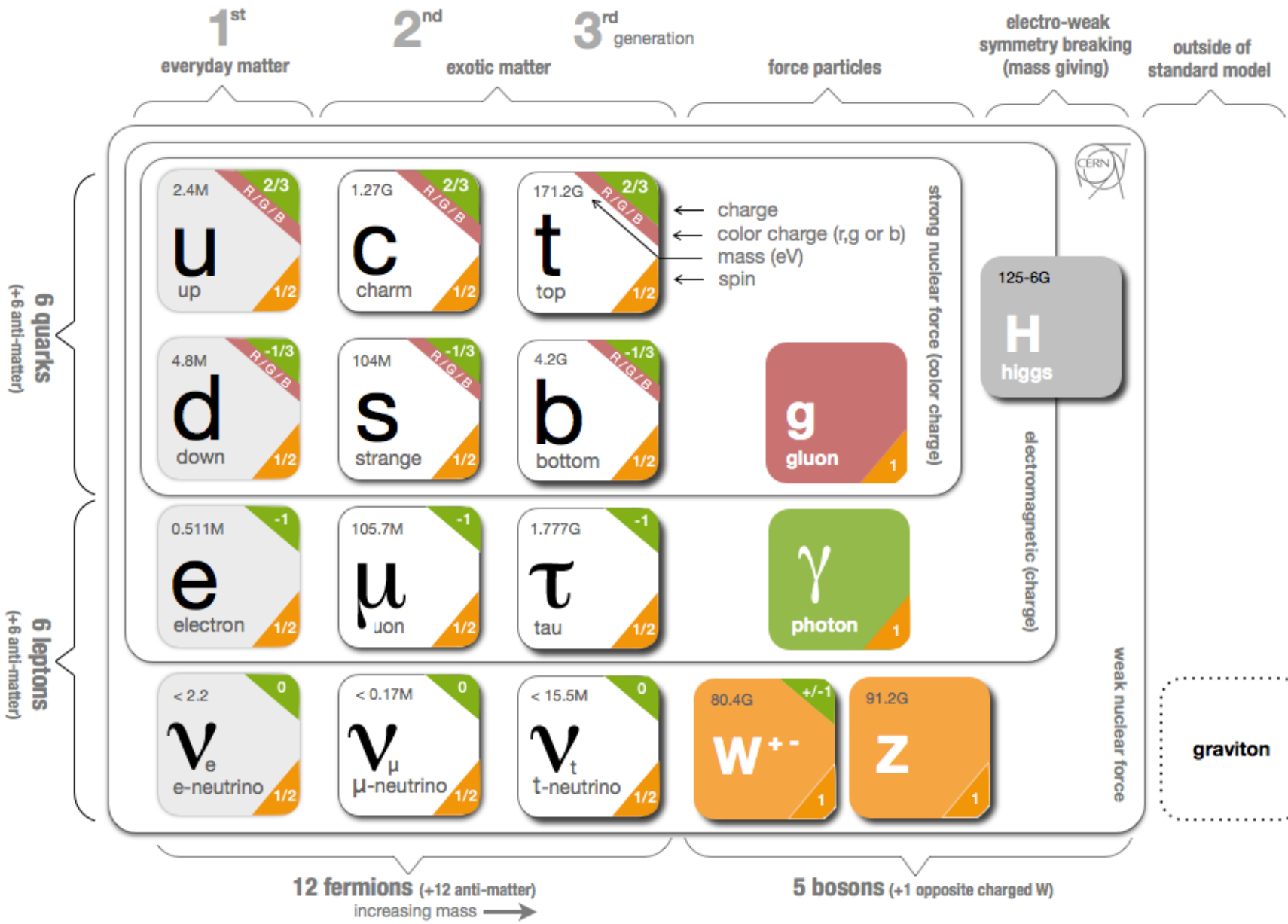


[Hier klicken](#) **Blick ins Buch!**



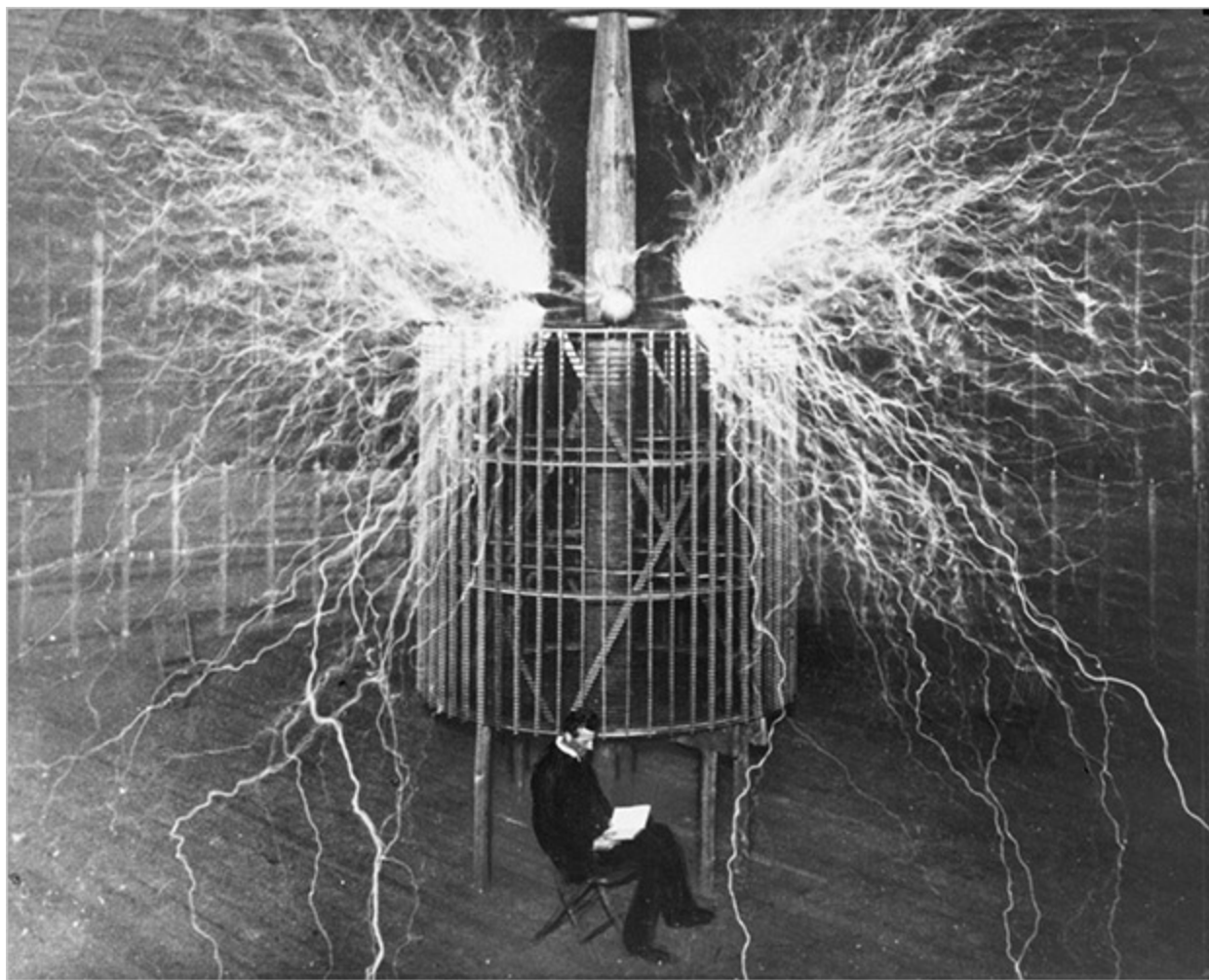
[Hier klicken](#) **Blick ins Buch!**





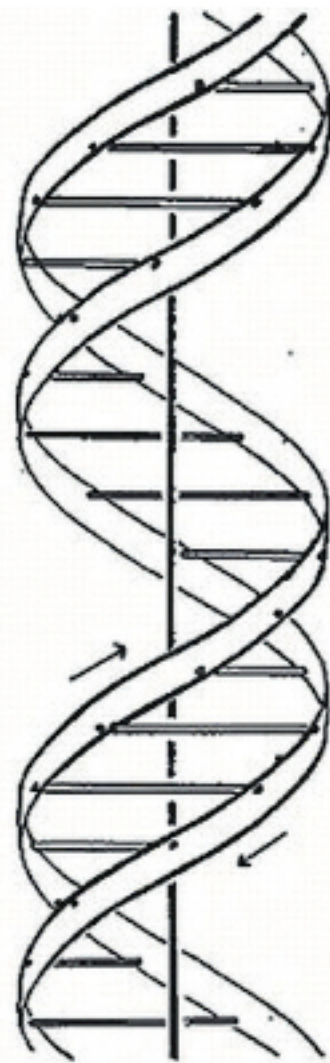
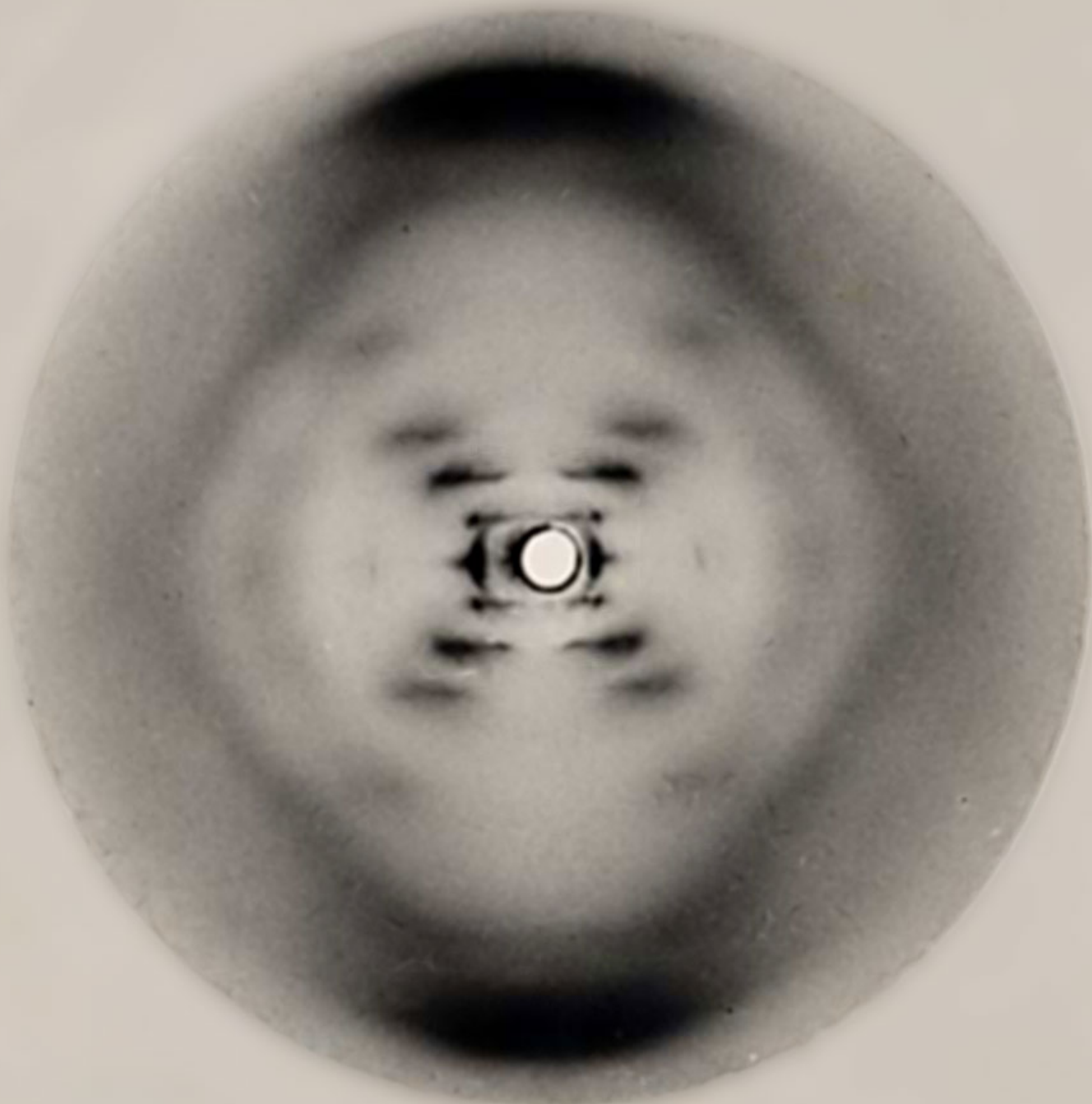
$$\begin{aligned}
\mathcal{L}_{GWS} = & \sum_f (\bar{\Psi}_f (i\gamma^\mu \partial_\mu - m_f) \Psi_f - e Q_f \bar{\Psi}_f \gamma^\mu \Psi_f A_\mu) + \\
& + \frac{g}{\sqrt{2}} \sum_i (\bar{a}_L^i \gamma^\mu b_L^i W_\mu^+ + \bar{b}_L^i \gamma^\mu a_L^i W_\mu^-) + \frac{g}{2c_w} \sum_f \bar{\Psi}_f \gamma^\mu (I_f^3 - 2s_w^2 Q_f - I_f^3 \gamma_5) \Psi_f Z_\mu + \\
& - \frac{1}{4} |\partial_\mu A_\nu - \partial_\nu A_\mu - ie(W_\mu^- W_\nu^+ - W_\mu^+ W_\nu^-)|^2 - \frac{1}{2} |\partial_\mu W_\nu^+ - \partial_\nu W_\mu^+ + \\
& - ie(W_\mu^+ A_\nu - W_\nu^+ A_\mu) + ig' c_w (W_\mu^+ Z_\nu - W_\nu^+ Z_\mu)|^2 + \\
& - \frac{1}{4} |\partial_\mu Z_\nu - \partial_\nu Z_\mu + ig' c_w (W_\mu^- W_\nu^+ - W_\mu^+ W_\nu^-)|^2 + \\
& - \frac{1}{2} M_\eta^2 \eta^2 - \frac{g M_\eta^2}{8 M_W} \eta^3 - \frac{g'^2 M_\eta^2}{32 M_W} \eta^4 + |M_W W_\mu^+ + \frac{g}{2} \eta W_\mu^+|^2 + \\
& + \frac{1}{2} |\partial_\mu \eta + i M_Z Z_\mu + \frac{ig}{2c_w} \eta Z_\mu|^2 - \sum_f \frac{g}{2} \frac{m_f}{M_W} \bar{\Psi}_f \Psi_f \eta
\end{aligned}$$

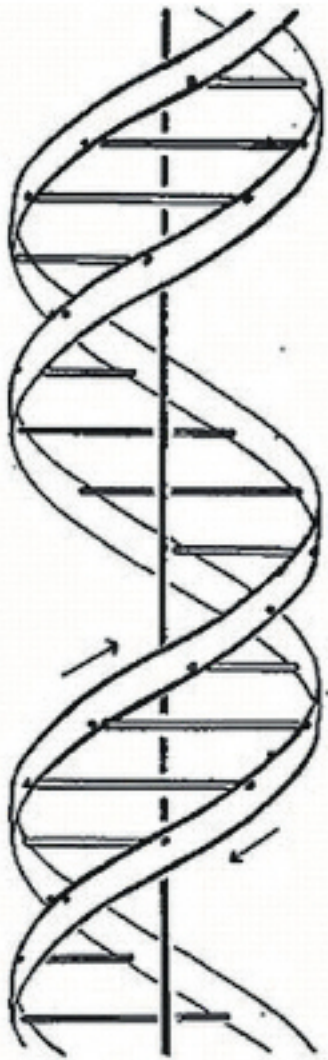




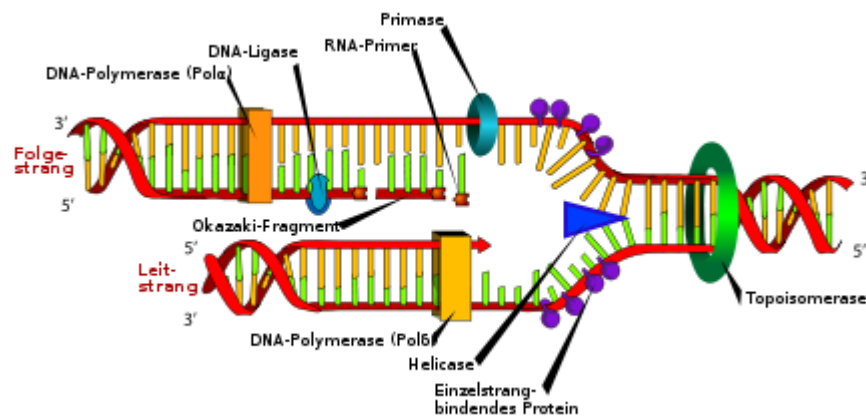


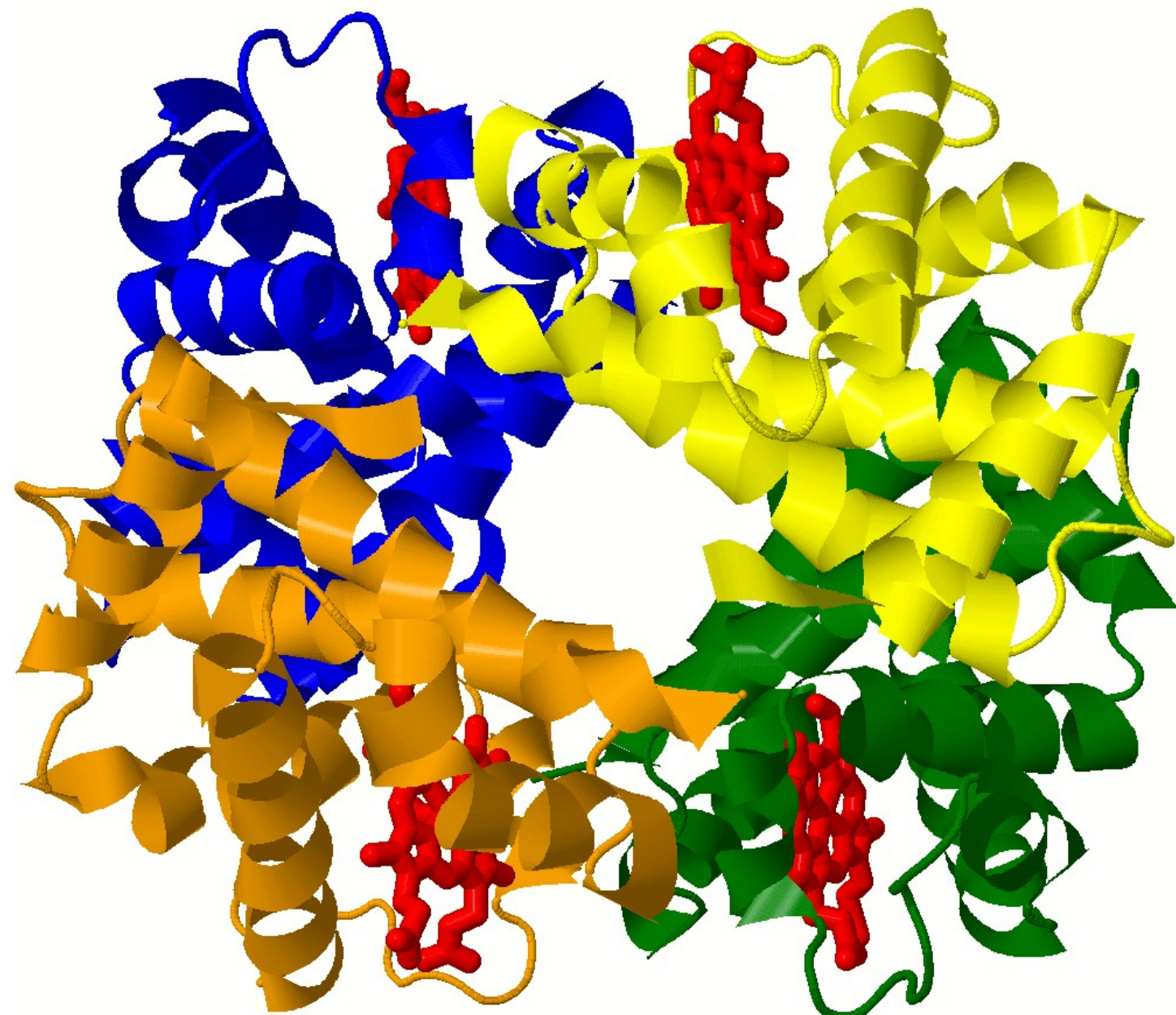
Chas
Adams

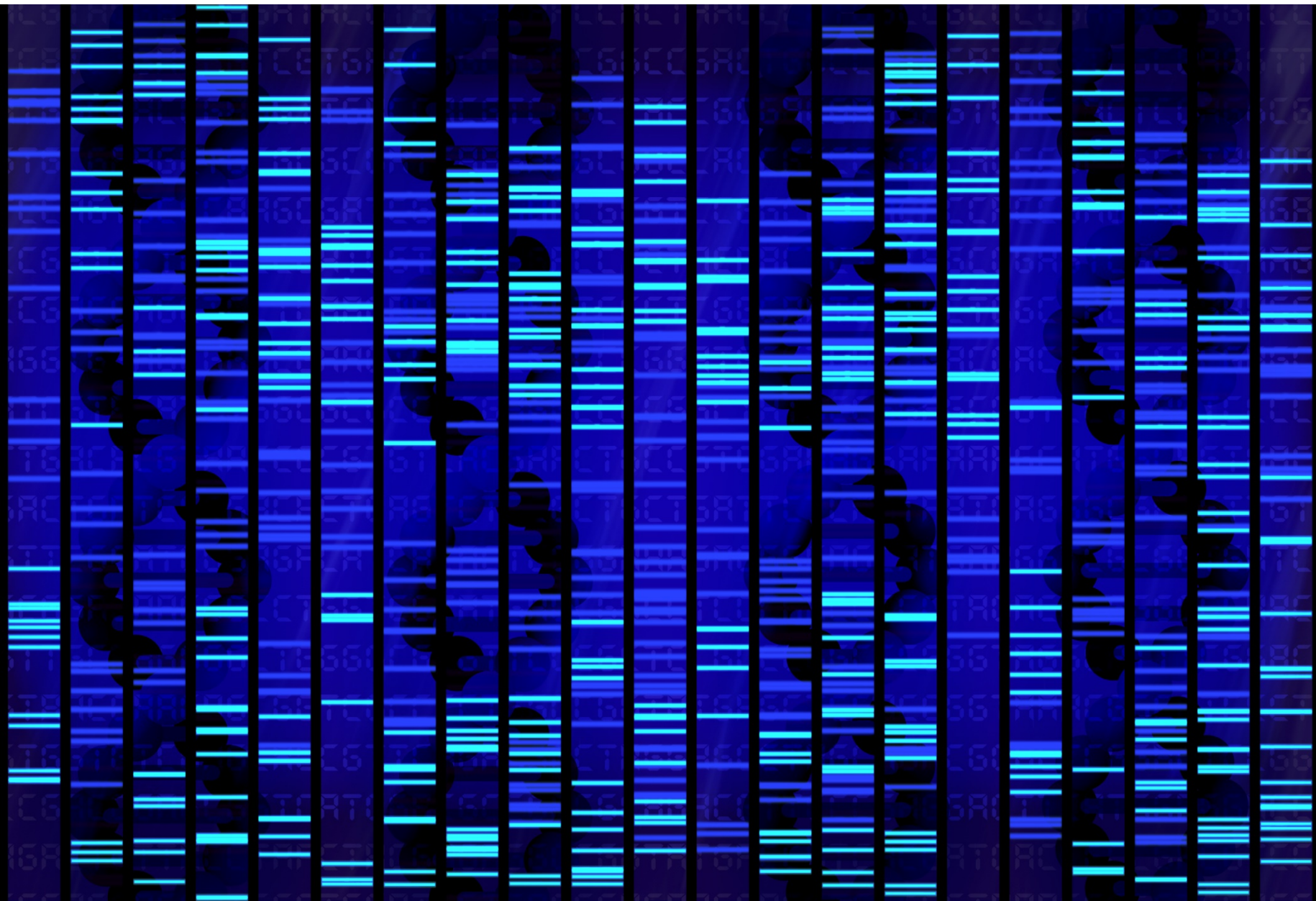


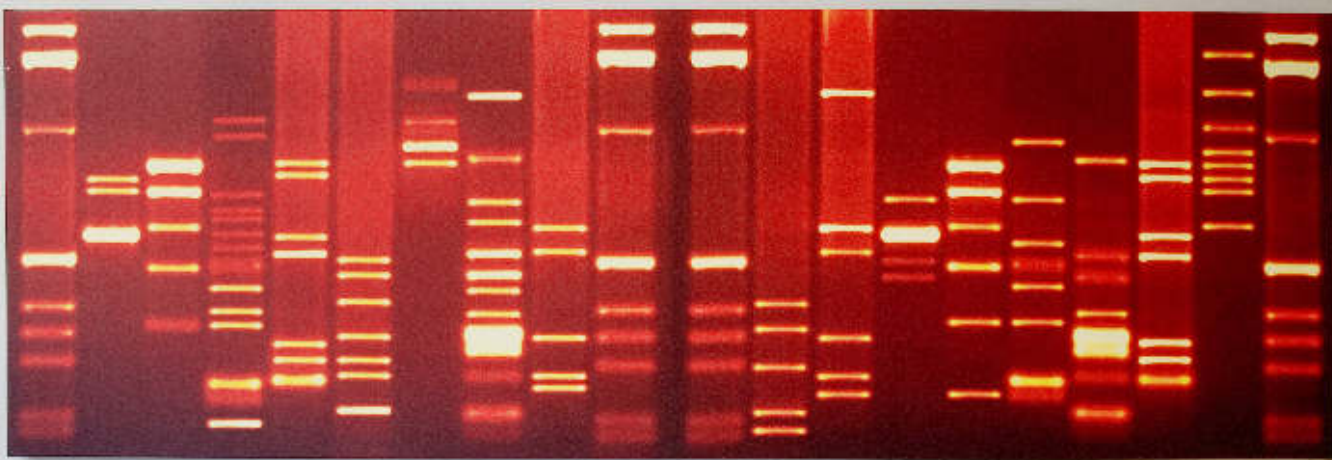


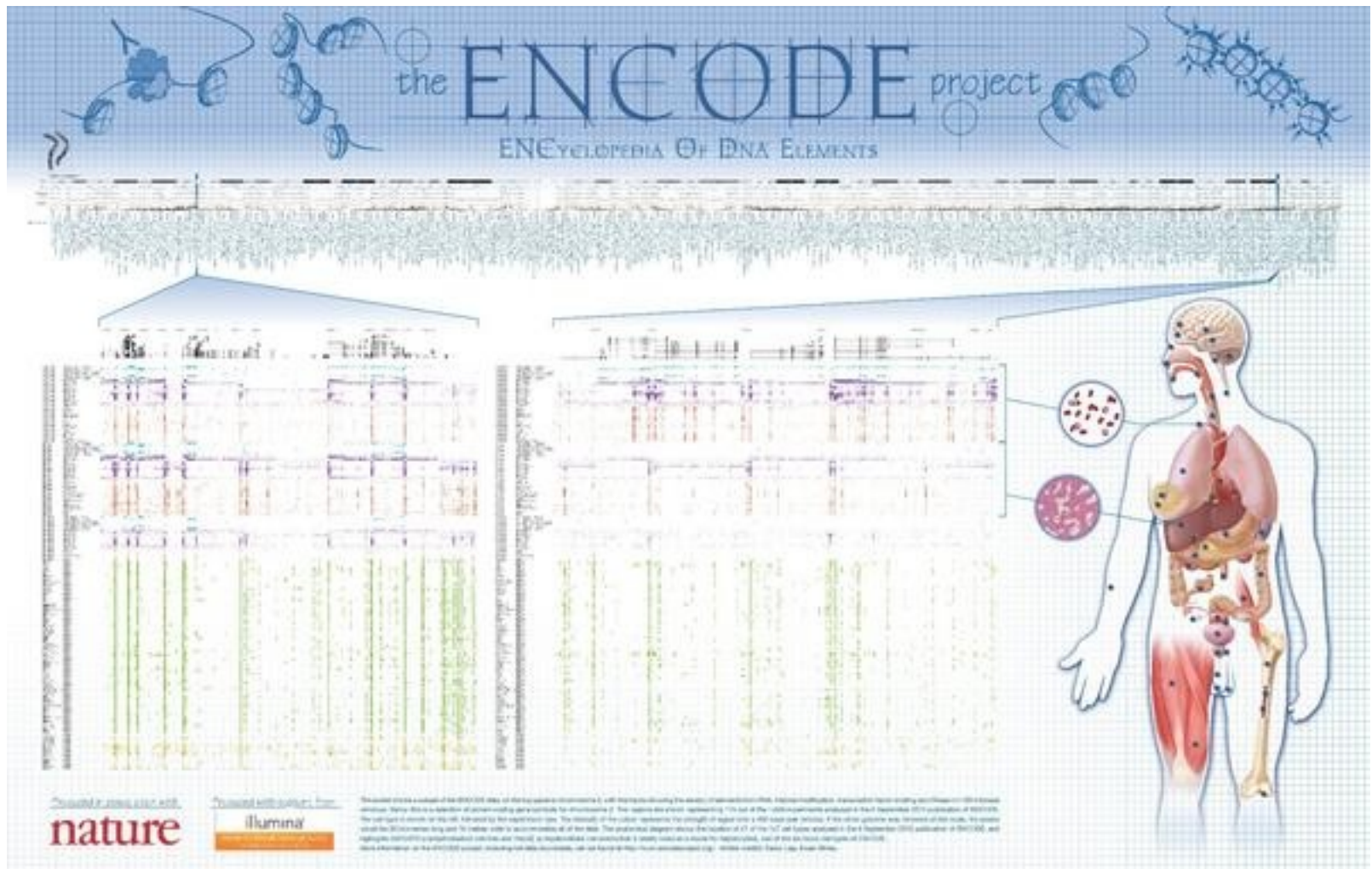
© R.G. Steane

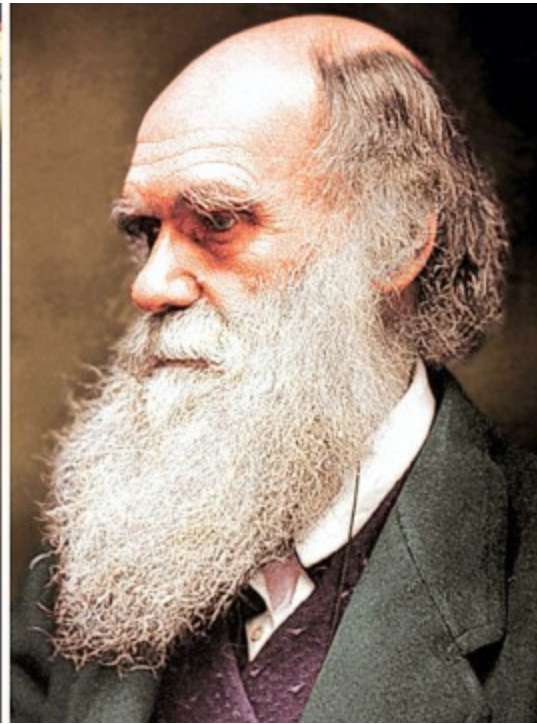
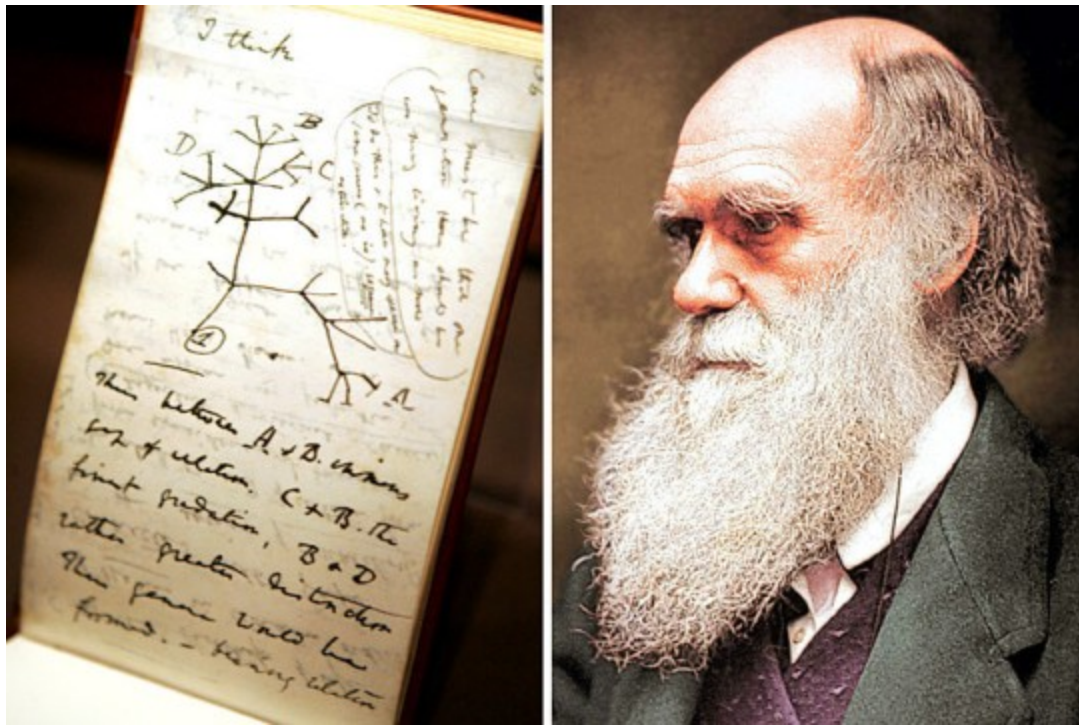




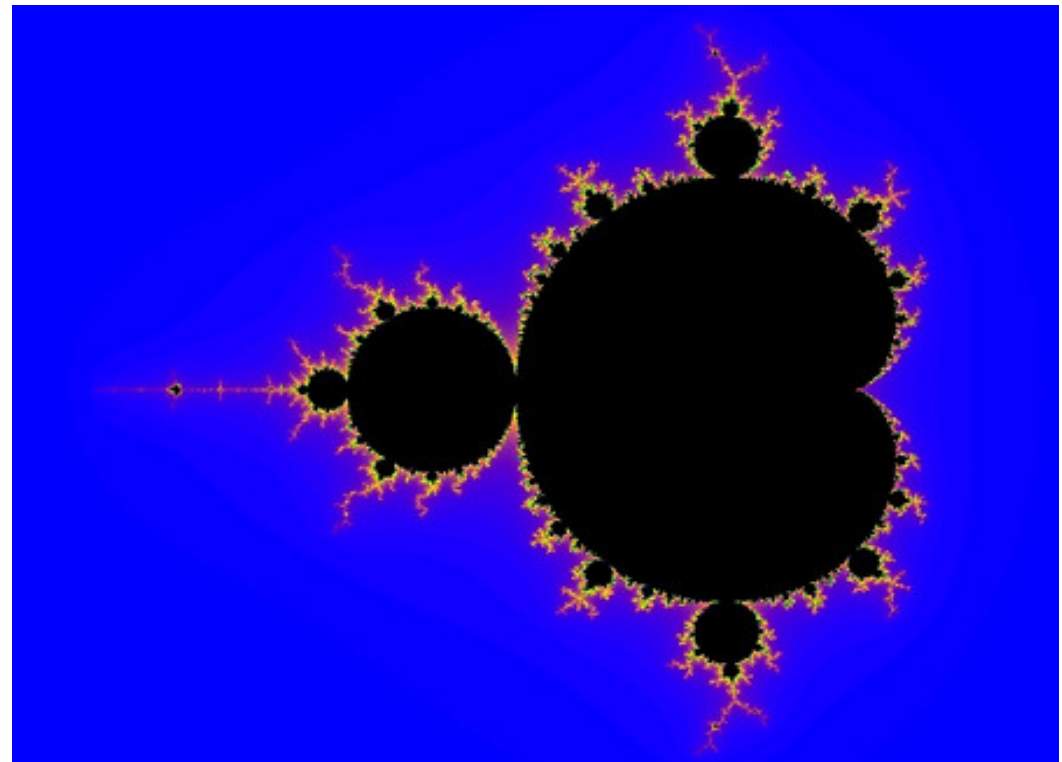




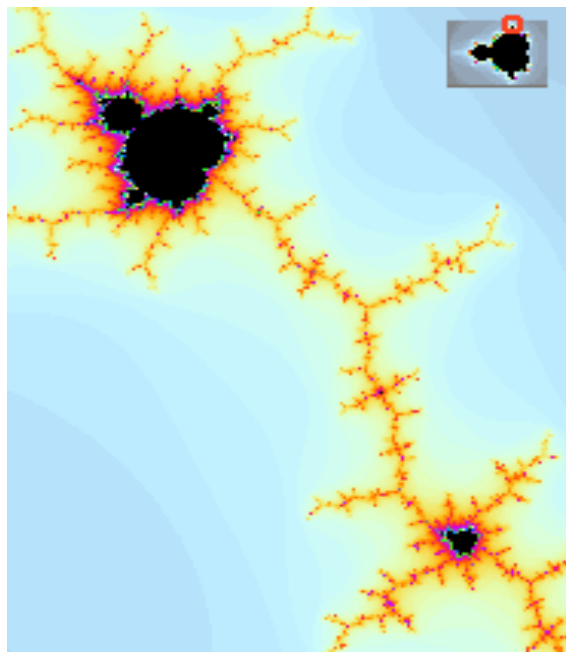




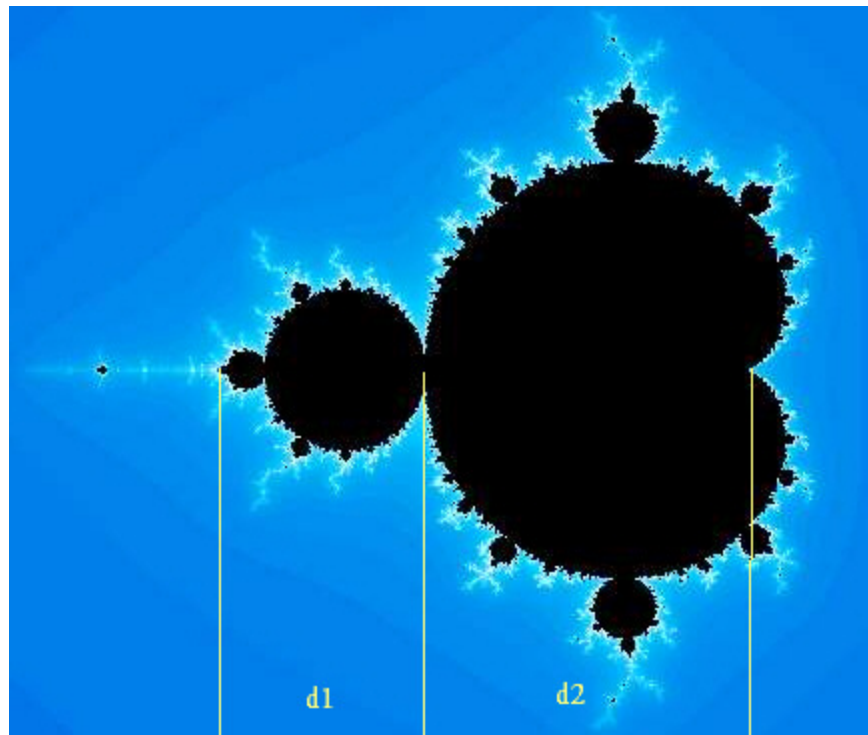
Benoit Mandelbrot



Ausschnitte des Mandelbrotfraktals



Mandelbrots Geigenkasten



Fraktale Figuren

